Title	On Lift of Delta Wings with Leading-Edge Vortices at Low Speeds
Author(s)	Hayashida, Nasahiro; Sato, Masayoshi; Matsuoka, Kenji
Editor(s)	
Citation	Bulletin of University of Osaka Prefecture. Series A, Engineering and natural sciences. 1978, 26(2), p.37-51
Issue Date	1978-03-31
URL	http://hdl.handle.net/10466/8287
Rights	

On Lift of Delta Wings with Leading-Edge Vortices at Low Speeds

Masahiro HAYASHIDA*, Masayoshi SATO** and Kenji MATSUOKA**

(Received November 15, 1977)

This paper is concerned with some aerodynamic lift characteristics of delta wings for supersonic aircraft.

With increasing aircraft speed, planform of a wing must change the geometry from the rectangular to the swept-back, further to the delta, and consequently aspect ratio of the wing tends to decrease.

For actual aircraft, however, aerodynamic performance of the wings at low speed is also important problem. Especially, improvement of STOL characteristics at low speed will much more be required. Therefore, problem of the lift augmentation of the delta wings at low speed has become more significant for supersonic aircraft.

In this paper, for reasonable vortex model of the delta wing, aerodynamic forces with leading-edge separation are analyzed theoretically and maximum value of the lift coefficient is also presented and discussed.

1. Introduction

The most remarkable point for lift characteristics of the delta wing is the appearance of the vortex lift in addition to the potential lift[1]. (See Fig. 1). The leading-edge vortices introduce the vortex lift and increase in intensity for chordwise. If the so-called vortex breakdown does not occur, these vortices will provide the stable lift, therefore, the

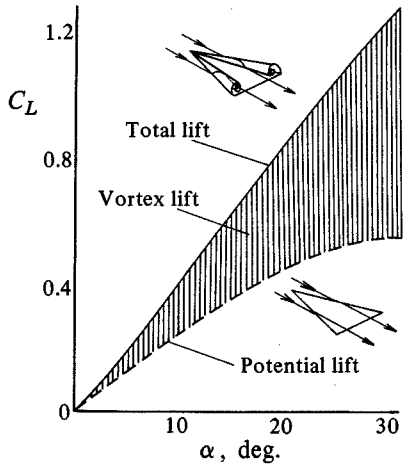

Fig. 1. Illustration of vortex lift for delta wing.

* Graduate Student, Department of Aeronautical Engineering, College of Engineering.
** Faculty, Department of Aeronautical Engineering, College of Engineering.

total lift will exceed the lift than the potential flow alone.

Only one paper[2] presents maximum lift of the wing with low aspect ratio. The paper discusses the core radius and distance apart of vortices with cores rolling up at infinitely long distance behind the wing as variations. Compared with its study which may be short of the availability in practical use, the present paper has a merit that the variation is limited to the circulation value around the mid-span of the wing.

2. Nomenclature

b = wing span.
b' = distance apart of the vortices rolling up at infinitely long distance behind the wing.
c = mid-wing chord length.
S = wing area.
λ = wing aspect ratio.
L = lift.
C_L = lift coefficient.
D_i = induced drag.
C_{D_i} = induced drag coefficient.
x = chordwise coordinate.
y = spanwise coordinate or real axis of the Trefftz plane.
z = imaginary axis of the Trefftz plane.
M = downward momentum of the two-dimensional fluid on the Trefftz plane.
E = total energy of the two-dimensional fluid on the Trefftz plane.
V = freestream velocity.
w' = down-wash velocity at infinitely long distance behind the wing. (considering the rolling up)
γ = vorticity.
γ_0 = chordwise mid-span vorticity.
Γ_0 = chordwise mid-span circulation.
ϵ'_∞ = down-wash angle at infinitely long distance behind the wing. (considering the rolling up)
ρ = fluid mass density.
φ = velocity potential.
n, ξ = variable constants which define the form of the vorticity distribution.
k = non-dimensional mid-span circulation, Γ_0/bV.

3. Theoretical analyses

Considering a Trefftz plane at infinitely long distance behind the wing, the lift and

induced drag on the wing are approximately given by the following relations[3),4)] by the momentum theory and energy law:

$$L = MV - E \sin \epsilon_\infty' , \tag{1}$$

and

$$D_i = E \cos \epsilon_\infty' . \tag{2}$$

In Appendix, the detailed introduction of these relations is presented.

Attention in application of the above equations is that, in the process of the rolling up from a flat surface of the trailing vortex sheet into a pair of vortices, the work which is performed by the pressure or the energy spent on rolling up is ignored. This approximation is general and allowed to use in practical problem[4),5)]. The values of M and E in Eqs. (1) and (2) are, in this discussion, presented by values of the momentum and energy calculated on the Trefftz plane for the case where the trailing vortex sheet keeps a flat surface at infinitely long distance behind the wing.

The present analysis can easily be extended for more practical case, in which the rolling up of the trailing vortex sheet is sufficiently considered.

3.1 Assumption of a basic vortex model

Some vortex models have been applied for the analysis of delta wings with leading-edge vortices. The vortex model presented by Gersten[6)], who assumed the free vortex sheets leave away from the upper surface of the wing with one-half the angle of attack as shown in Fig. 2, agrees well with experimental measurements. To overcome the very

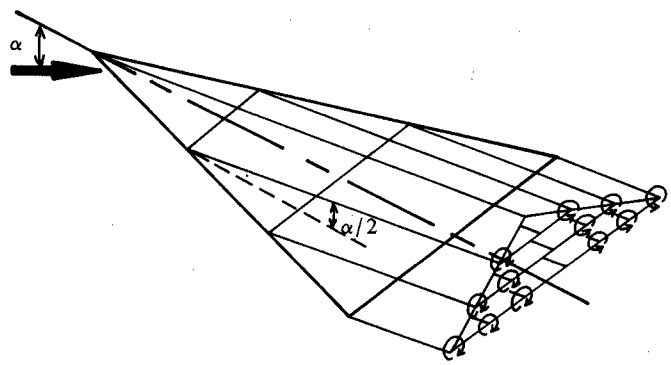

Fig. 2. Nonlinear vortex model by Gersten.

complex analysis by the above model, we will begin with the assumption of a basic vortex model for simplicity.

The form of pressure distribution on the delta wing at high angle of attack shall first be investigated on the basis of some concrete experimental data. As shown in

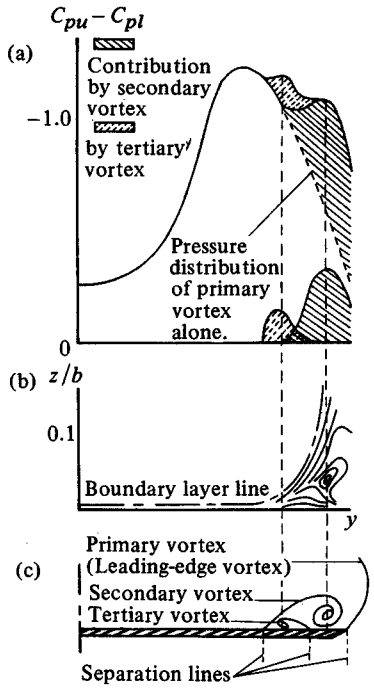

Fig. 3. Experimental pressure distribution.
a) Pressure distribution of difference between upper's *Cpu* and lower's *Cpl*.
b) Total pressure distribution.
c) Flow pattern. (diagrammatic)

Fig. 3[7], the spanwise pressure distribution is of U-shape or has the curve which is nearly elliptical from the mid-span to the outside and takes the negative peak at the point between about 60 and 70% semi-span. The negative pressure decreases outwards from the peak point and becomes zero at the wingtip (that is, the leading edge for the delta wing). The stronger leading-edge vortex (primary vortex) is, the greater the contributions induced by the secondary and tertiary vortices are, and therefore, the change in the outside stated above will not be so much. This tendency suggests that the pressure distribution can be approximated as elliptical form from the mid-span to the peak point and as constant from that point to the wingtip.

The distribution of vorticity on the wing can approximately be expressed by the following equations as shown in Fig. 4:

$$\gamma(x,y) = \begin{cases} \gamma_0 \left[1+n-n\sqrt{1-\dfrac{y^2}{(\frac{\xi b x}{2c})^2}} \right] & (0 \leqq |y| \leqq \dfrac{\xi b x}{2c}), \quad (3) \\ \gamma_0 (1+n) & (\dfrac{\xi b x}{2c} \leqq |y| \leqq \dfrac{b x}{2c}). \quad (4) \end{cases}$$

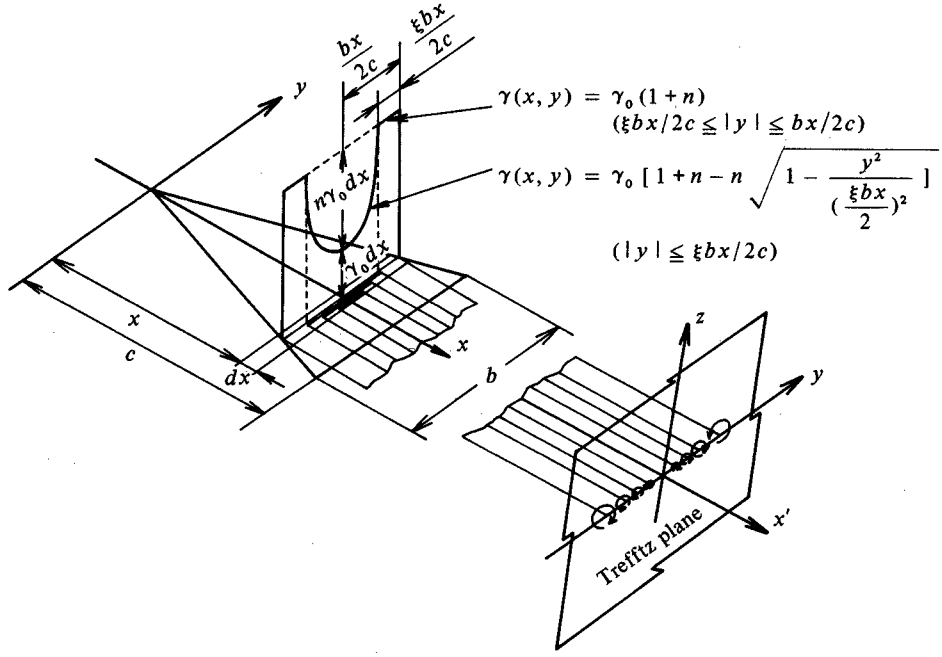

Fig. 4. Basic vortex model and Trefftz plane at infinitely long distance behind the wing. (considering the leading-edge separation)

3.2 Momentum on Trefftz plane

Consider the vortex arrangement formed by the free vortices on the Trefftz plane. Since the vortices of the strength given by

$$\frac{\partial [\gamma(x, y)dx]}{\partial y}$$

leave away from a wing element dx, it consists of vortices which are shed from the section $0 \leqq |y| \leqq \xi bx/2c$ and a pair of point vortices from the both tips ($|y| = bx/2c$). The vortices shed from the section $\xi bx/2c < |y| < bx/2c$ do not exist.

It is well known that the momentum of the fluid whose flow is induced by a pair of point vortices of the same strength but the opposite directions in the two-dimensional infinitely wide plane will have the finite value $\rho \ell \Gamma$[8], where ρ is the fluid mass density, ℓ is the distance between two point vortices and Γ is the strength of circulation of each point vortex. This relation yields

$$dM = -\int_0^{bx/2c} \rho \cdot 2y \cdot \frac{\partial}{\partial y} [\gamma(x, y)dx]\, dy$$

$$= \frac{\rho\gamma_0 b}{c} [1 + (1 - \frac{\pi\xi}{4})n]\, x\,dx, \tag{5}$$

where dM denotes the elementary momentum depended on the wing element. Thus the total downward ($-z$ direction in Fig. 4) momentum M on the Trefftz plane is

$$M = \int_{x=0}^{x=c} dM = \frac{1}{2}\left[1 + \left(1 - \frac{\pi\xi}{4}\right)n\right] \rho b \Gamma_0 . \tag{6}$$

3.3 Energy on Trefftz plane

The kinetic energy for two-dimensional incompressible fluid is given by

$$E = -\frac{1}{2}\rho \oint \varphi \cdot \frac{\partial \varphi}{\partial n'} ds' \quad ^{9)}, \tag{7}$$

where s' represents the length along a boundary line and n' does the direction of the normal line put on a boundary line.

In the calculation of E with Eq. (7), the Trefftz plane is regarded as a $y - z$ complex plane and the value of E in the whole infinitely wide $y - z$ plane is obtained by doubling the value integrated on the half infinitely wide $y - z$ plane. After integrating along the path $A \to B \to C \to D \to E \to F \to A$ as shown in Fig. 5, the limits of $R \to +\infty$

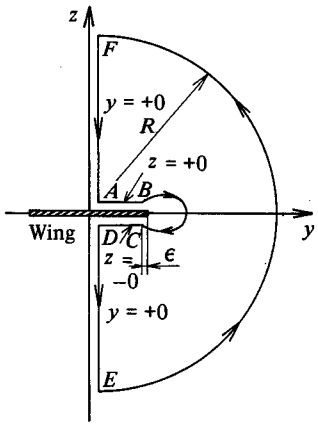

Fig. 5. Path of line integration.
($B \to C$, $D \to E$, $F \to A$; along one of stream lines)

and $\epsilon \to 0$ are operated. As the velocity potential φ is finite and z-axis and the path $B \to C$ are stream lines, we have

$$\left(\varphi \cdot \frac{\partial \varphi}{\partial n'}\right)_{\substack{B\to C \\ D\to E \\ F\to A}} = 0,$$

which results in $E_{B\to C} = E_{D\to E} = E_{F\to A} = 0$. Since the fluid can be regarded as stationary at the limit of $R \to +\infty$ about the path $E \to F$, the formula of $E_{E\to F} = 0$ and otherwise

$$E_{A\to B} = \lim_{\epsilon\to 0}\left(-\frac{\rho}{2}\int_{+0}^{\frac{b}{2}-\epsilon}\left(\varphi \cdot \frac{\partial \varphi}{\partial z}\right)_{z=+0} dy\right),$$

and

$$E_{C\to D} = \lim_{\epsilon\to 0}\left(-\frac{\rho}{2}\int_{\frac{b}{2}-\epsilon}^{+0}\left(\varphi\cdot\frac{\partial\varphi}{\partial z}\right)_{z=-0}\cdot(-dy)\right).$$

Generally, the product $[\varphi\cdot(\partial\varphi/\partial z)]_{z=\pm 0}$ can be rewritten as the expression $(\varphi)_{z=\pm 0}\cdot(\partial\varphi/\partial z)_{z=\pm 0}$. And, considering the condition of the vortex sheet, the quantity $(\varphi)_{z=+0}$ is equal to $-(\varphi)_{z=-0}$ and $(\partial\varphi/\partial z)_{z=+0}$ is also to $-(\partial\varphi/\partial z)_{z=-0}$. These situations disclose that the value $E_{A\to B}$ is equal to $E_{C\to D}$. The finite value of energy on the Trefftz plane can be finally expressed by

$$E = 2\lim_{\substack{\epsilon\to 0\\ R\to+\infty}}\left(E_{A\to B}+E_{B\to C}+E_{C\to D}+E_{D\to E}+E_{E\to F}+E_{F\to A}\right)$$

$$= -2\rho\int_0^{b/2}(\varphi)_{z=+0}\cdot\left(\frac{\partial\varphi}{\partial z}\right)_{z=+0}dy\,. \tag{8}$$

In the calculation of the value of E by Eq. (8), the quantity of $(\varphi)_{z=+0}$ and $(\partial\varphi/\partial z)_{z=+0}$ are required which are to be calculated in what follows.

3.3.1 Calculation of $(\varphi)_{z=+0}$

A complex potential $df(\zeta)$ on the Trefftz plane due to the vortices which leave away from the wing element is

$$df(\zeta) = \int_{-b/2c}^{+b/2c}\frac{\dfrac{\partial}{\partial y}[\gamma(x,y)dx]}{2\pi i}\log(\zeta-y)dy\,, \tag{9}$$

where $\zeta = y+iz$ and

$$\frac{\partial}{\partial y}[\gamma(x,y)dx] = \begin{cases} \dfrac{n\gamma_0}{\left(\frac{\xi bx}{2c}\right)}\cdot\dfrac{y}{\sqrt{\left(\frac{\xi bx}{2c}\right)^2-y^2}}dx & \left(0\leqq y\leqq\dfrac{\xi bx}{2c}\right),\\ 0 & \left(\dfrac{\xi bx}{2c}<y<\dfrac{bx}{2c}\right),\\ (n+\gamma_0)dx & \left(y\geqq\dfrac{bx}{2c}\right). \end{cases}$$

Hence, the elementary velocity potential $d\varphi$ is

$$d\varphi = \mathrm{Re}\,[df(\zeta)]$$

$$= -\frac{n\gamma_0 dx}{\left(\frac{\xi bx}{c}\right)}\left[\left[\left(y-\frac{\xi bx}{2c}\right)^2+z^2\right]\left[\left(y+\frac{\xi bx}{2c}\right)^2+z^2\right]\right]^{1/4}\sin\frac{\theta_1+\theta_2}{2}$$

$$+\frac{n\gamma_0 dx}{\left(\frac{\xi bx}{c}\right)}z+\frac{(n+1)\gamma_0 dx}{2\pi}(\theta_1-\theta_2), \tag{10}$$

where

$$\theta_1 = \tan^{-1} \frac{z}{y - \frac{\xi bx}{2c}} \quad \text{and} \quad \theta_2 = \tan^{-1} \frac{z}{y + \frac{\xi bx}{2c}} .$$

The necessary quantity $(\varphi)_{z=+0}$ is obtained by using the relation

$$(\varphi)_{z=+0} = \int_{x=0}^{x=c} d(\varphi)_{z=+0} .$$

The limiting form of Eq. (10) as $z \to +0$ becomes

$$d(\varphi)_{z=+0} = \begin{cases} -\dfrac{n\gamma_0 dx}{(\frac{\xi bx}{c})} \sqrt{(\frac{\xi bx}{2c})^2 - y^2} + \dfrac{(n+1)\gamma_0 dx}{2} & (0 \leqq y \leqq \dfrac{\xi bx}{2c}), \\ \dfrac{(n+1)\gamma_0 dx}{2} & (\dfrac{\xi bx}{2c} \leqq y \leqq \dfrac{bx}{2c}), \\ 0 & (y > \dfrac{bx}{2c}). \end{cases} \tag{11}$$

Therefore, $(\varphi)_{z=+0}$ can be obtained as follows by integrating $d(\varphi)_{z=+0}$ with x for each section of x :

$$(\varphi)_{z=+0} = \begin{cases} -\dfrac{n\gamma_0}{(\frac{\xi b}{c})} [\sqrt{(\frac{\xi b}{2})^2 - y^2} - y \cos^{-1}(\frac{2y}{\xi b}) + \dfrac{(n+1)\gamma_0}{(\frac{\xi b}{c})} (\frac{b}{2} - y)] & \\ & (0 \leqq y \leqq \dfrac{\xi b}{2}), \\ \dfrac{(n+1)\gamma_0}{(\frac{b}{c})} (\frac{b}{2} - y) & (\dfrac{\xi b}{2} \leqq y \leqq \dfrac{b}{2}). \end{cases} \tag{12}$$

3.3.2 Calculation of $(\partial\varphi/\partial z)_{z=+0}$

Similarly to the above, $(\partial\varphi/\partial z)_{z=+0}$ is obtained through

$$d(\frac{\partial\varphi}{\partial z})_{z=+0} = \begin{cases} \dfrac{n\gamma_0 dx}{(\frac{\xi bx}{c})} + \dfrac{(n+1)\gamma_0 dx}{2\pi} (\dfrac{1}{y - \frac{bx}{2c}} - \dfrac{1}{y + \frac{bx}{2c}}) & (0 \leqq y \leqq \dfrac{\xi bx}{2c}), \\ -\dfrac{n\gamma_0 dx}{(\frac{\xi bx}{c})} \dfrac{y}{\sqrt{y^2 - (\frac{\xi bx}{2c})^2}} + \dfrac{n\gamma_0 dx}{(\frac{\xi bx}{c})} & \\ + \dfrac{(n+1)\gamma_0 dx}{2\pi} (\dfrac{1}{y - \frac{bx}{2c}} - \dfrac{1}{y + \frac{bx}{2c}}) & \\ & (y > \dfrac{\xi bx}{2c}), \end{cases} \tag{13}$$

such that

$$\left(\frac{\partial\varphi}{\partial z}\right)_{z=+0}=\begin{cases}\dfrac{n\gamma_0}{\left(\frac{\xi b}{c}\right)}\log\left(\dfrac{\xi b}{4y}\right)-\dfrac{(n+1)\gamma_0}{\left(\frac{b}{c}\right)\pi}\log\left[\left(\dfrac{b}{2y}\right)^2-1\right] & \left(0\leqq y\leqq\dfrac{\xi b}{2}\right),\\ \dfrac{n\gamma_0}{\left(\frac{\xi b}{c}\right)}\left[\log\left(1+\sqrt{1+\left(\dfrac{\xi b}{2y}\right)^2}\right)-\log 2\right] & \\ \qquad -\dfrac{(n+1)\gamma_0}{\left(\frac{b}{c}\right)\pi}\log\left[\left(\dfrac{b}{2y}\right)^2-1\right] & \left(\dfrac{\xi b}{2}<y\leqq\dfrac{b}{2}\right).\end{cases}\tag{14}$$

3.3.3 Calculated value of E[10)]

The total energy E may now be calculated by substituting Eqs. (13) and (14) into Eq. (8) as

$$E=\rho\Gamma_0^2\left[\frac{n^2}{16}\pi+\frac{(n+1)^2}{2\pi}\left[(2-\xi)\log\xi+\frac{2}{\xi}\log 2\right]+n(n+1)\left[\left(\frac{5-3\xi}{4\xi}\right)\log 2\right.\right.$$
$$\left.\left.+\left(\frac{\xi}{4}\right)\log\xi+\frac{5\xi-11}{8\xi}-\left(\frac{\xi^2+2}{4\xi}\right)\log\left(1+\sqrt{1-\xi^2}\right)+\frac{3\sqrt{1-\xi^2}}{4\xi}\right]\right].\tag{15}$$

3.4 Estimation of the down-wash angle ϵ_∞' at infinitely long distance behind the wing

The distance b' apart of the vortices, which can approximately be regarded as a pair of point vortices, is given by equating the momentum in the case to Eq. (6) as follows:

$$b'=\frac{1}{2}\left[1+\left(1-\frac{\xi\pi}{4}\right)n\right]b.\tag{16}$$

Under this consideration, the down-wash velocity w' at infinitely long distance behind the wing is approximately

$$w'=\frac{\Gamma_0}{2\pi b'}=\frac{\Gamma_0}{\pi\left[1+\left(1-\frac{\xi\pi}{4}\right)n\right]b}.\tag{17}$$

Hence, the down-wash angle ϵ_∞' at infinitely long distance behind the wing can approximated by

$$\epsilon_\infty'=\sin^{-1}\frac{w'}{V}=\sin^{-1}\frac{\Gamma_0}{\pi\left[1+\left(1-\frac{\xi\pi}{4}\right)n\right]bV}.\tag{18}$$

3.5 Estimations of lift and induced drag coefficients

Since the lift on the wing is given by Eq. (1), the lift coefficient is

$$C_L = \frac{L}{\frac{1}{2}\rho V^2 S} = Ak\left(1 - \frac{2B}{\pi A}k^2\right)\lambda ,$$

where

$$A = 1 + \left(1 - \frac{\xi\pi}{4}\right)n ,$$

and

$$B = \frac{\pi}{16}n^2 + (n+1)^2 \frac{(2-\xi)\log\xi + \frac{2}{\xi}\log 2}{2\pi}$$

$$+ n(n+1)\left[\frac{5-3\xi}{4\xi}\log 2 + \frac{\xi}{4}\log\xi + \frac{5\xi - 11}{8\xi}\right.$$

$$\left. - \left(\frac{\xi^2+2}{4\xi}\right)\log\left(1+\sqrt{1-\xi^2}\right) + \frac{3\sqrt{1-\xi^2}}{4\xi}\right] .$$

Then, we obtain

$$\frac{C_L}{\lambda} = Ak\left(1 - \frac{2B}{\pi A^2}k^2\right), \tag{19}$$

and its maximum value is given by

$$\left(\frac{C_L}{\lambda}\right)_{max} = \frac{2}{3}A^2\sqrt{\frac{\pi}{6B}} , \tag{20}$$

at

$$k = A\sqrt{\frac{\pi}{6B}} . \tag{21}$$

Similarly the induced drag coefficient being

$$C_{D_i} = \frac{D_i}{\frac{1}{2}\rho V^2 S} = 2Bk^2\sqrt{1 - \frac{k^2}{\pi^2 A^2}}\,\lambda ,$$

we have

$$\frac{C_{D_i}}{\lambda} = 2Bk^2\sqrt{1 - \frac{k^2}{\pi^2 A^2}} . \tag{22}$$

3.6 Estimation of variable constants ξ and n

The value given by Eqs. (19), (20) and (22) contain the variable constants ξ and n whose values have to be estimated. With respect to ξ, the value of ξ may be between $\xi = 0.6$ and 0.7 on the strength of many experimental data for the delta wing which have already been published. The case of $\xi = 1.0$ corresponds to such a case as the flow on

the wing is potential flow alone.

With respect to n, it can be allowed that the potential flow is realized in the section $0 \leqq |y| \leqq \xi bx/2c$ as shown in Fig. 3 (b) and (c). Thus the value of n can be determined by equivalent substitution of area according to Jones' theory[11] as shown in Fig. 6. In Jones' theory, the distribution of the vorticity on the wing is given by

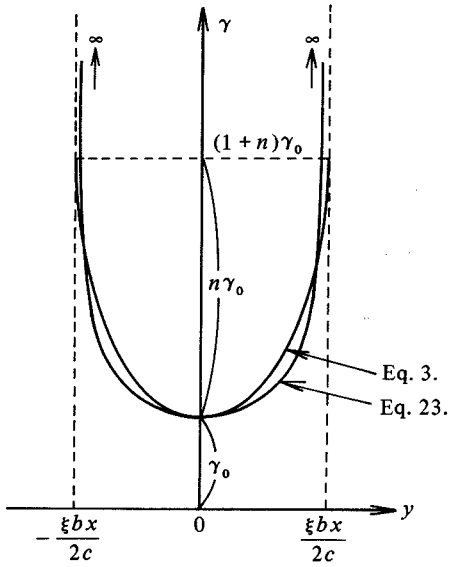

Fig. 6. Estimation of constant n.

$$\gamma(x, y) = \frac{\gamma_0}{\sqrt{1 - \dfrac{y^2}{(\dfrac{\xi bx}{2c})^2}}} \tag{23}$$

The comparison of this with the above equation and Eq. (3) for the equivalent substitution of area gives the following relation:

$$\int_{-\xi bx/2c}^{\xi bx/2c} \frac{\gamma_0}{\sqrt{1 - \dfrac{y^2}{(\dfrac{\xi bx}{2c})^2}}}\, dy = \int_{-\xi bx/2c}^{\xi bx/2c} \gamma_0 \left[1 + n - n\sqrt{1 - \frac{y^2}{(\frac{\xi bx}{2c})^2}}\right] dy. \tag{24}$$

Hence, the value of n is obtained as

$$n = \frac{\dfrac{\pi}{2} - 1}{1 - \dfrac{\pi}{4}} \fallingdotseq 2.660\,. \tag{25}$$

4. Results and conclusions

Introducing the value $n = 2.660$ into Eqs. (19), (20) and (22), the final results of the lift and induced drag coefficients, and the maximum lift coefficient for each case of $\xi = 0.6$, 0.7 and 1.0 become

$$\left.\begin{aligned} \frac{C_L}{\lambda} &= 2.407\,k\,(1-0.102\,k^2) \\ \frac{C_{D_i}}{\lambda} &= 1.849\,k^2\sqrt{1-0.0180\,k^2} \\ C_{Lmax} &= 2.906\,\lambda \end{aligned}\right\} \quad \text{at } \xi = 0.6, \tag{26}$$

$$\left.\begin{aligned} \frac{C_L}{\lambda} &= 2.198\,k\,(1-0.0988\,k^2) \\ \frac{C_{D_i}}{\lambda} &= 1.498\,k^2\sqrt{1-0.0210\,k^2} \\ C_{Lmax} &= 2.692\,\lambda \end{aligned}\right\} \quad \text{at } \xi = 0.7, \tag{27}$$

$$\left.\begin{aligned} \frac{C_L}{\lambda} &= 1.571\,k\,(1-0.1077\,k^2) \\ \frac{C_{D_i}}{\lambda} &= 0.8350\,k^2\sqrt{1-0.0411\,k^2} \\ C_{Lmax} &= 1.842\,\lambda \end{aligned}\right\} \quad \text{at } \xi = 1.0. \tag{28}$$

Eqs. (26), (27) and (28) are summerized with non-dimensional mid-span circulation k in Fig. 7.

In Fig. 7, the curve for $\xi = 1.0$ represents the case without the leading-edge separation, that is, the flow on the wing is the potential flow alone[12]. The difference (the shaded area) between the curve for $\xi = 1.0$ and that for $\xi = 0.6$ or 0.7 may be regarded as the vortex lift which depends on the leading-edge separation. The contribution of this vortex lift reaches about 40 ~ 50% of the potential lift at that maximum value.

The total lift has the maximum value as well as the case of the potential lift, and that value may be limited about 2.5 ~ 3 times of the wing aspect ratio. In the case that the leading-edge separation is considered, the leading-edge vortices give an effective lift as the additional lift. Therefore, it may be expected that if the leading-edge separation is made positively and these leading-edge vortices are maintained by some methods (such as blowing or suction, etc.), the lift coefficient will attain to the theoretical value which is predicted in this paper.

The results obtained here may be used as the available data for the investigation of the lift augmentation of delta wing.

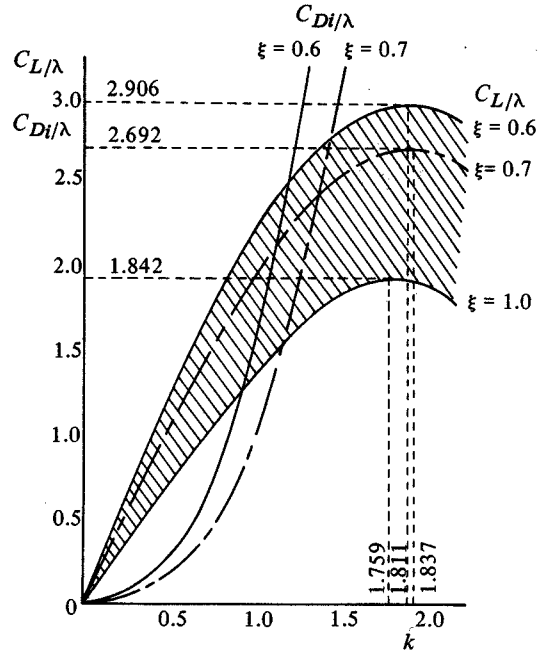

Fig. 7. Variations of C_L/λ and C_{Di}/λ with k.
(for each case of $\xi = 0.6$, 0.7 and 1.0 at $n = 2.660$)

References

1) E. C. Polhamas, J. of Aircraft, **8**, 193 (1971).
2) D. W. Bridson et al., Aero. J. of RAS, **74**, 671 (1970).
3) L. Prandtl, Tragflügertheorie, (1919).
4) H. B. Helmbold, J. Aero. Sci., **24**, 237 (1957).
5) J. R. Spreiter et al., J. Aero. Sci., **18**, 21 (1951).
6) K. Gersten, Ing. Arch., **30**, 431 (1961).
7) D. Hummel, Z. Flugwiss., **15**, 355 (1967).
8) B. Fujimoto, Ryutairikigaku (rev. ed.), p.65, Yokendo, Tokyo (1965).
9) W. F. Durand, Aerodynamic Theory (1), p.86, Dover Publications, New York (1963).
10) D. Bierens De Haan, Nouvelles Tables (D'Integrales Définies), De L'academic Royale des Sciences, Amsterdam.
11) R. T. Jones, NACA TR. **835**, 59 (1946).
12) M. Sato, J. of JSAS, **21**, 563 (1973).
13) H. Schlichting et al., Aerodynamik des Flugzeuges (2), **81**, Springer-Verlag, Berlin (1960).
14) D. Hummel, Z. Flugwiss., **13**, 158 (1965).
15) H. Ludwieg, Z. Flugwiss., **10**, 242 (1962).
16) K. Kraemer, Z. Flugwiss., **10**, 297 (1962).
17) J. F. Campbell, J. of Aircraft, **13**, 727 (1976).
18) R. G. Bradley et al., J. of Aircraft, **11**, 33 (1974).
19) G. J. Hancock, Aero. J. of RAS, **74**, 749 (1970).

Appendix: Estimations of lift and induced drag by Trefftz plane approach method

Consider an infinitely large cylinder which includes the wing inside as the control surface as shown in Fig. 8 (a).

The force F on the wing can be given as

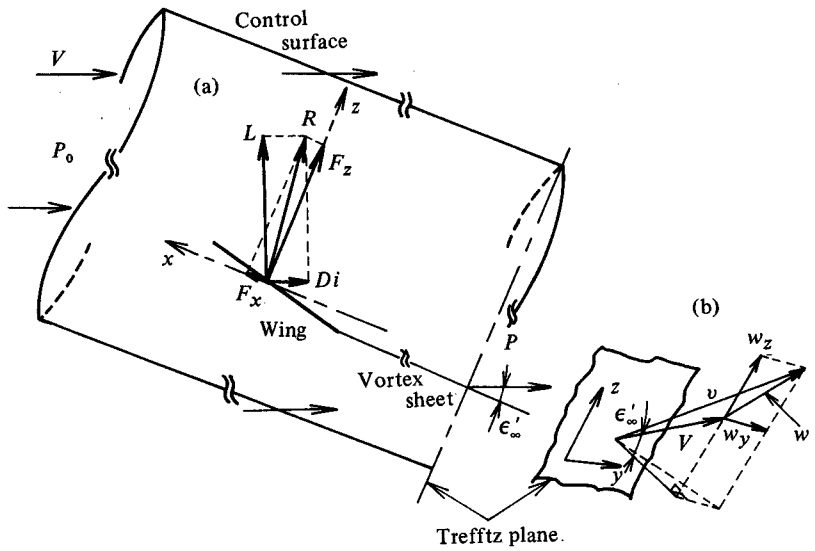

Fig. 8. Control surface.
a) Coordinate system and forces on wing.
b) Resultant velocity at Trefftz plane.

$$\boldsymbol{F} = \boldsymbol{P} - \boldsymbol{G},$$

where $\boldsymbol{P}$ is the pressure integral value over the control surface and $\boldsymbol{G}$ is the effluent momentum out of the control surface per unit time. Now, the cylinder radius being infinitely long, the difference of momentum between incomings and outgoings through the surrounding surface of the cylinder will be zero, and P_z, z-component of $\boldsymbol{P}$, will be also zero. Finally, $\boldsymbol{P}$ and $\boldsymbol{G}$ will have only to be considered with respect to the infinitely wide front and rear planes of the cylinder. The latter plane is so-called Trefftz plane. Consequently, the following equation will be obtained with respect to the force in the z-direction :

$$F_z = P_z - G_z = MV\cos\epsilon'_\infty \ ,$$

where M is the momentum in the direction to $(-z)$ on the Trefftz plane. While, since

$$F_z = L\cos\epsilon'_\infty + D_i \sin\epsilon'_\infty \ ,$$

we obtain

$$L\cos\epsilon'_\infty + D_i \sin\epsilon'_\infty = MV\cos\epsilon'_\infty \ . \qquad \text{(A.1)}$$

On the other hand, as shown in Fig. 8 (b) the resultant velocity v at an arbitrary point on the Trefftz plane can be expressed by

$$v^2 = V^2 + 2Vw_z \sin\epsilon'_\infty + w^2,$$

where w is the induced velocity due to a straight free vortices row on the Trefftz plane and w_z is the z-component of it. Denoting the pressure at the front and rear (in other words, the Trefftz's) plane of the cylinder by P_0 and P, respectively, the x-component of $\boldsymbol{P}$ becomes

$$\begin{aligned} P_x &= \iint (P - P_0)\,dy\,dz \\ &= \iint \frac{1}{2}\rho(V^2 - v^2)\,dy\,dz \\ &= V \sin \epsilon_\infty' \iint \rho(-w_z)\,dy\,dz - \iint \frac{1}{2}\rho w^2\,dy\,dz \quad . \\ &= MV \sin \epsilon_\infty' - E. \end{aligned}$$

As obviously $G_x = 0$, the following equation will secondly be obtained with respect to the force in the x-direction:

$$F_x = P_x - G_x = MV \sin \epsilon_\infty' - E\,.$$

On the other hand, we have

$$F_x = L \sin \epsilon_\infty' - D_i \cos \epsilon_\infty'\,.$$

Therefore, we obtain

$$L \sin \epsilon_\infty' - D_i \cos \epsilon_\infty' = MV \sin \epsilon_\infty' - E\,. \tag{A.2}$$

From Eqs. (A.1) and (A.2), accordingly, the lift L and the induced drag D_i are given by

$$L = MV - E \sin \epsilon_\infty'\,,$$

and

$$D_i = E \cos \epsilon_\infty'\,,$$

which correspond to Eqs. (1) and (2). Moreover the latter equation can also be obtained by the energy law only.